

Order α_s^2 magnetic penguin correction for B decay to light mesons

C. S. Kim^a and Yeo Woong Yoon^b

^a*Department of Physics and IPAP, Yonsei University, Seoul 120-749, Korea*

^b*School of Physics, KIAS, Seoul 130-722, Korea*

E-mail: cskim@yonsei.ac.kr, ywoon@kias.re.kr

ABSTRACT: We compute the order α_s^2 correction to the matrix element of magnetic penguin operator for B meson decaying to light mesons within the QCD factorization framework. We explicitly show that the soft and collinear divergences are canceled out, so that the validity of QCD factorization is confirmed. We present the result of the calculation in complete analytic forms. The result is also applied to $B \rightarrow K\pi$ decays, and we find that the order α_s^2 correction of magnetic penguin operator can considerably reduce the coefficient of penguin amplitude $a_{4,I}^c$. The reduction is stronger for the imaginary part.

KEYWORDS: B -physics, QCD factorization, NLO computations

ARXIV EPRINT: [1107.1601](https://arxiv.org/abs/1107.1601)

Contents

1	Introduction	1
2	Formalism	3
3	Soft, Collinear and UV divergence	6
3.1	Soft and collinear divergence cancelation	6
3.2	Renormalization - UV divergence cancelation	9
4	Result and application	10
5	Conclusions	15
A	Appendix: Analytic formulae of the master integrals	15

1 Introduction

Non-leptonic B decays have great affluence of phenomenological applications. Especially, they provide a plenty of fascinating CP asymmetries in the standard model (SM), where we have a number of chances to test the SM by searching discrepancies between the theoretical predictions and experimental measurements. The measurements of CP asymmetries have been performed well in various B factories such as Belle and BaBar and also in Tevatron. Furthermore, upcoming B factories such as LHC-b, Super-B and Belle-2 will shed more light on CP asymmetries by accumulating much larger amount of data.

For a long time, $B \rightarrow K\pi$ decays have been a continuously engrossing issue due to that some puzzling behavior occurs in their CP asymmetry measurements: The difference between $A_{CP}(\pi^\mp K^\pm)$ and $A_{CP}(\pi^0 K^\pm)$ measured by Belle, BaBar and CDF collaborations is unexpectedly larger than the theoretical estimates [1–4] in the SM. Recent brand-new result from the LHC-b experiment also supports the behavior [5]. There have been numerous new physics analyses on the issue model-independently or model-dependently. However, before we explore new physics effects beyond the SM to resolve the puzzle, it is strongly required that one should perform more precise higher order corrections to the observables within the SM.

The QCD factorization (QCDF) is a theoretical framework for systematically calculating hadronic matrix element of weak decays of B meson [6]. It has been extensively applied to non-leptonic B decays [7–9]. The QCDF formalism for hadronic matrix element

of non-leptonic B decays is described by

$$\begin{aligned} \langle M_1 M_2 | Q_i | B \rangle &= \sum_j F_j^{B \rightarrow M_1}(m_2^2) f_{M_2} \int_0^1 du T_{ij}^I(u) \Phi_{M_2}(u) + (M_1 \leftrightarrow M_2) \\ &+ f_B f_{M_1} f_{M_2} \int_0^1 d\xi du dv T_i^{II}(\xi, u, v) \Phi_B(\xi) \Phi_{M_1}(v) \Phi_{M_2}(u), \end{aligned} \quad (1.1)$$

where $F^{B \rightarrow M_i}$ is $B \rightarrow M_i$ form-factor, f_{M_i} is decay constant of meson M_i , and $\Phi_{M_i}(u)$ is light-cone distribution amplitude of meson M_i with parton momentum fraction u . The formalism is expressed by convolution of hard-scattering kernel $T^{I,II}$ with meson distribution amplitude at the leading power of Λ_{QCD}/m_b . The hard-scattering kernel is separated into the hard-scattering form-factor term T^I and the hard-scattering spectator term T^{II} . The very first paper of QCDF calculated next-to-leading order (NLO) correction to $B \rightarrow \pi\pi$ decays [6]. The imaginary part of the decay amplitude, which causes strong CP phase, arises first at the order α_s from hard-scattering contribution between decaying quarks of different mesons. Therefore, the next-to-next-to leading order (NNLO) correction is of great importance in perturbative expansion in order to provide reliable prediction for CP asymmetries.

The NNLO correction to tree amplitude for hard-scattering form-factor term has been calculated first for imaginary part [10] and later for real part [11], where the order α_s^2 contribution is quite significant compared to the order α_s contribution. Especially, the color-suppressed amplitude is very sensitive to the order α_s^2 contribution. The result is also confirmed by ref. [12]. As for the hard-scattering spectator term, the one-loop order α_s^2 correction has been calculated for tree amplitude [13–15] and for penguin amplitude [16, 17]. However, the order α_s^2 penguin correction for the hard-scattering form-factor term has not yet been calculated. This correction is more important for $B \rightarrow K\pi$ decays because the tree amplitudes are CKM-suppressed and the decays are penguin-dominant. Especially, the order α_s^2 penguin correction is highly required for theoretical estimate of CP asymmetries since it is the first correction in perturbative expansion.

Motivated by current status of higher order correction for B to light meson decays, here we compute the order α_s^2 one-loop contribution (NLO) for the magnetic penguin operator as the first step toward the complete order α_s^2 correction of penguin amplitude. In section 2, we describe the formalism for the calculation. In order to regularize ultra-violet (UV) divergences and infra-red (IR) divergences in the NLO calculation, we use dimensional regularization where the space-time dimension d is analytically continued to $d = 4 - 2\varepsilon$. Especially, we choose naive dimensional regularization (NDR) scheme for the prescription of γ_5 . We use 't Hooft-Feynman gauge ($\xi = 1$) throughout the calculation. In section 3, we explicitly show that the soft and collinear divergences are canceled out in the calculation. The result of calculation is expressed in section 4 in complete analytic forms. We relegate our analytic results of the master integrals to appendix. We apply our result to $B \rightarrow K\pi$ decays and provide numerical values of the NLO correction for magnetic penguin operator compared with other contributions. In section 5, we summarize and conclude.

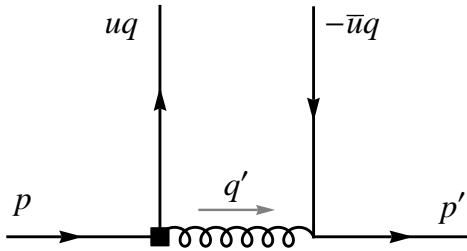


Figure 1. Order α_s (LO) diagram for magnetic penguin operator with momentum configuration. $\bar{u} = 1 - u$ is understood. The square box denotes Q_{8g} insertion.

2 Formalism

The effective amplitude of non-leptonic weak decays of B meson, such as $B \rightarrow M_1 M_2$, is expressed [18] by

$$A_{eff} = \frac{G_F}{\sqrt{2}} \sum_i \lambda^i C_i(\mu) \langle M_1 M_2 | Q_i | B \rangle(\mu) \quad (2.1)$$

with effective operators Q_i , $i = 1, 2, \dots, 10, 7\gamma, 8g$. G_F is Fermi constant and λ^i is a factor for CKM matrix elements corresponding to operator Q_i . The magnetic penguin operator Q_{8g} , on which we are focusing in this work, is defined by

$$Q_{8g} = -\frac{g_s}{8\pi^2} m_b \bar{s} \sigma_{\mu\nu} (1 + \gamma_5) G^{\mu\nu} b, \quad (2.2)$$

where $G^{\mu\nu}$ is gluonic field strength tensor contracted by SU(3) generators. We do not consider the magnetic γ -penguin operator $Q_{7\gamma}$ because the contribution is much suppressed by the fine-structure constant. The Wilson coefficients $C_i(\mu)$ are to be calculated near weak boson mass scale M_W where we can safely avoid large logarithms in perturbative expansion. Then, $C_i(\mu)$ are evolved into m_b scale through renormalization group equation associated with anomalous dimension matrix. In principle, the scale dependence of $C_i(\mu)$ should be canceled by the scale dependence of the full calculation of matrix element $\langle M_1 M_2 | Q_i | B \rangle(\mu)$ up to the order of truncation of perturbative expansion.

The calculation of hadronic matrix element can be handled within the QCDF framework. The formalism is expressed in eq. (1.1). In this framework soft gluon exchange between decaying quarks is power suppressed in heavy quark limit. The dominant hard gluon scattering contribution is absorbed into hard-scattering kernels $T^{I,II}$. The matrix element is described by convolution of hard-scattering kernel with meson distribution amplitude. Basically, T^I starts at order unity in perturbative expansion, while T^{II} starts at order α_s . It should be noted that the contribution of magnetic penguin operator in T^I starts at order α_s . In order word, leading order (LO) diagram for magnetic penguin operator is order α_s as shown in figure 1. This property is same with all other penguin amplitudes. In the figure 1, spectator quark line is suppressed. Left horizontal line denotes incoming b quark with momentum p and right horizontal line is outgoing quark with momentum p' which forms a bound state of a meson with spectator anti-quark. The upper side lines represent the quark and anti-quark that make a bound state of another meson

with momentum q . u and \bar{u} (equal to $1 - u$) is parton momentum fraction of each quark in the upper side meson. The kinematic relations among the momentum four vectors are as follow:

$$p^2 = m_b^2, \quad q^2 = 0, \quad p'^2 = 0, \quad q'^2 = \bar{u}m_b^2, \\ p \cdot q = p \cdot p' = p' \cdot q = q \cdot q' = \frac{m_b^2}{2}, \quad p' \cdot q' = \frac{\bar{u}m_b^2}{2}, \quad p \cdot q' = \frac{(1 + \bar{u})m_b^2}{2}. \quad (2.3)$$

In order to obtain hard-scattering kernel T (superscript I is suppressed) for magnetic penguin operator, we use the QCDF formula which is schematically described by

$$\langle Q_{8g} \rangle_{\text{ren}} = F \cdot T \otimes \Phi_M, \quad (2.4)$$

where the symbol \otimes denotes convolution with meson distribution amplitude. $\langle Q_{8g} \rangle_{\text{ren}}$ is renormalized matrix element which is related with its bare quantity by

$$\langle Q_{8g} \rangle_{\text{ren}} = Z_m Z_g Z_q Z_G^{1/2} Z_{88} \langle Q_{8g} \rangle_0, \quad (2.5)$$

where Z_{88} is operator renormalization constant for Q_{8g} , and Z_m , Z_g , Z_q , Z_G are the mass, coupling, quark field and gluon field renormalization constant, respectively. The one-loop calculation of Z_{88} is shown in ref. [19]. We summarize each value of one-loop renormalization constant:

$$Z_m^{(1,1)} = -3C_F, \\ Z_g^{(1,1)} = -\frac{11}{6}N_c + \frac{1}{3}n_f, \\ Z_q^{(1,1)} = -C_F, \\ Z_{88}^{(1,1)} = 8C_F - 2N_c, \quad (2.6)$$

where the following power expansion is considered

$$Z_i = 1 + \sum_{j=1}^{\infty} \sum_{k=1}^j \left(\frac{\alpha_s}{4\pi} \right)^j \frac{1}{\varepsilon^k} Z_i^{(j,k)}. \quad (2.7)$$

Each quantity in the factorization formula eq. (2.4) can be power expanded. Since $\langle Q_{8g} \rangle_{\text{ren}}$ as well as T start at order α_s , we describe

$$\langle Q_{8g} \rangle_{\text{ren}} = \left(\frac{\alpha_s}{4\pi} \right) \left(\langle Q_{8g} \rangle_{\text{ren}}^{(0)} + \left(\frac{\alpha_s}{4\pi} \right) \langle Q_{8g} \rangle_{\text{ren}}^{(1)} + \mathcal{O}(\alpha_s^2) \right), \\ F = F^{(0)} + \left(\frac{\alpha_s}{4\pi} \right) F^{(1)} + \mathcal{O}(\alpha_s^2), \\ \Phi_M = \Phi_M^{(0)} + \left(\frac{\alpha_s}{4\pi} \right) \Phi_M^{(1)} + \mathcal{O}(\alpha_s^2), \\ T = \left(\frac{\alpha_s}{4\pi} \right) \left(T^{(0)} + \left(\frac{\alpha_s}{4\pi} \right) T^{(1)} + \mathcal{O}(\alpha_s^2) \right). \quad (2.8)$$

From the power expansion of factorization formula eq. (2.4), we obtain

$$\langle Q_{8g} \rangle_{\text{ren}}^{(0)} = T^{(0)}, \quad (2.9)$$

$$\langle Q_{8g} \rangle_{\text{ren}}^{(1)} = F^{(0)} T^{(1)} \otimes \Phi_M^{(0)} + F^{(1)} T^{(0)} \otimes \Phi_M^{(0)} + F^{(0)} T^{(0)} \otimes \Phi_M^{(1)}. \quad (2.10)$$

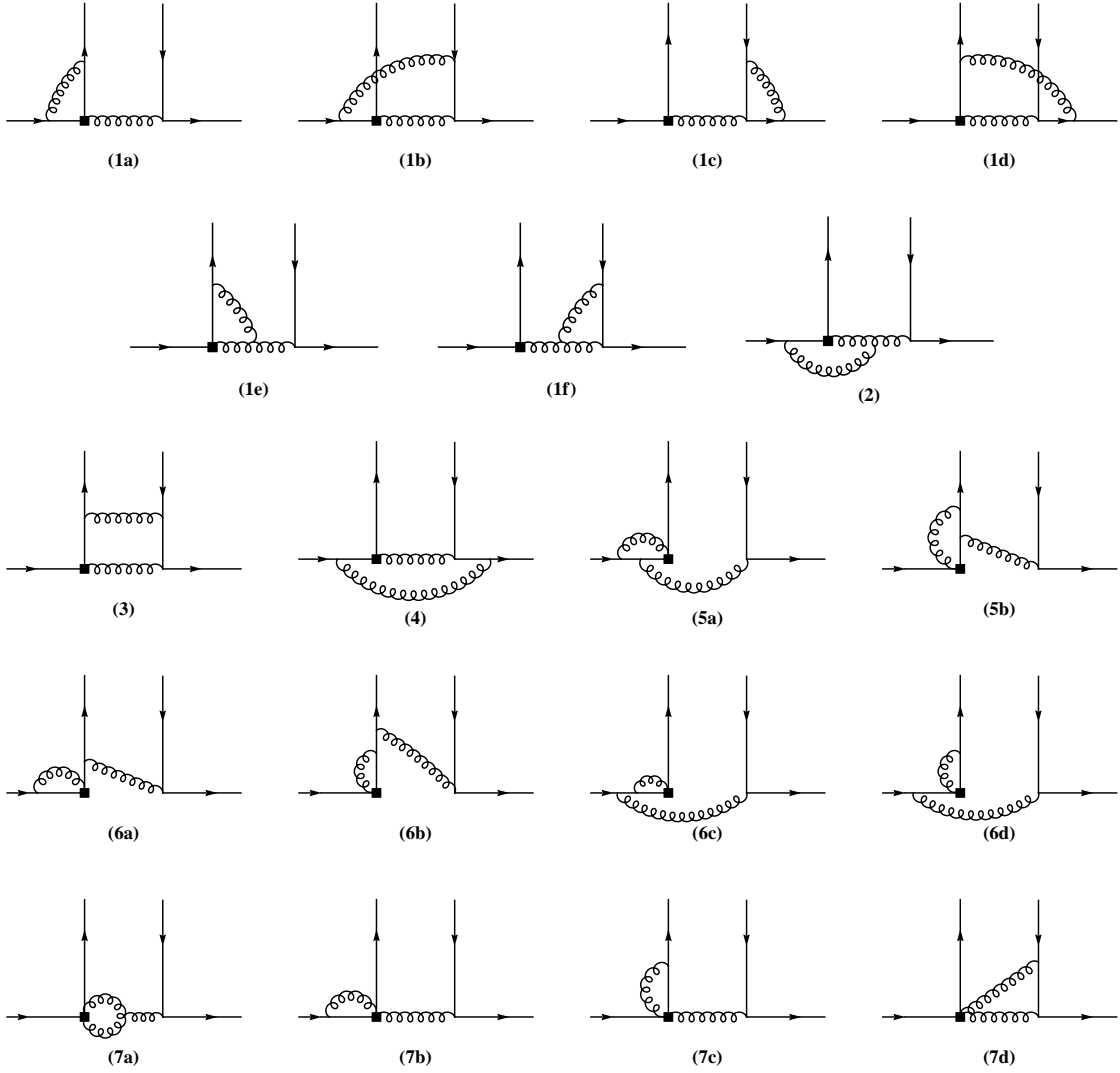


Figure 2. NLO diagrams for magnetic penguin operator. The momentum configurations for all the diagrams are same as in figure 1. The square box denotes Q_{sg} insertion.

Those eqs. (2.9,2.10) are the master formula for the calculating hard-scattering kernels. In those formula, all the quantities are renormalized while they might have IR divergences: All the IR divergences should be canceled in those equations. In the next section it will be explicitly shown that the soft and collinear divergences are canceled out in those equations. The NLO diagrams for magnetic penguin operator are shown in figure 2.

In order to compensate scale dependence of NLO hadronic matrix element, we have to employ next-to-leading logarithmic (NLL) Wilson coefficients for the Q_{sg} . We refer to refs. [20, 21] for NLL effective Wilson coefficient C_{sg}^{eff} at low energy scale. The light-cone projection operator of a light pseudoscalar meson in momentum space is applied to upper

side quark and anti-quark spinors. The projection operator in leading twist is given by

$$M_{\alpha\beta}^P = \frac{if_P}{4N_c} [\not{q}\gamma_5]_{\alpha\beta} \Phi_M(u), \quad (2.11)$$

where α, β are spinor indices of upper side quark and anti-quark spinors. The distribution amplitude of meson M denoted by $\Phi_M(u)$ is conventionally expanded in Gegenbauer polynomials:

$$\Phi_M(u, \mu) = 6u(1-u) \left[1 + \sum_{n=1}^{\infty} \alpha_n^M(\mu) C_n^{(3/2)}(2u-1) \right]. \quad (2.12)$$

$\alpha_n^M(\mu)$ are Gegenbauer moments and $C_n^{(3/2)}$ are Gegenbauer polynomials of order $\frac{3}{2}$. We truncate the expansion by $n = 2$. In order to consistently compensate NLO hadronic matrix element, we also use NLL evolution equation for Gegenbauer moments which are obtained in [22–24]:

$$\begin{aligned} \alpha_n^M(\mu) &= U_{nn} \alpha_n^M(\mu_0) + \delta_{n,2} U_{20}, \\ U_{nn} &= \left(\frac{\alpha_s(\mu_0)}{\alpha_s(\mu)} \right)^{\frac{\gamma_n^{(0)}}{2\beta_0}} \left[1 + \left(\frac{\gamma_n^{(1)}}{2\beta_0} - \frac{\gamma_n^{(0)}\beta_1}{2\beta_0^2} \right) \frac{\alpha_s(\mu_0) - \alpha_s(\mu)}{4\pi} \right], \\ U_{20} &= \left(\frac{\alpha_s(\mu)}{4\pi} \right) \left[1 - \left(\frac{\alpha_s(\mu_0)}{\alpha_s(\mu)} \right)^{1+\frac{\gamma_2^{(0)}}{2\beta_0}} \frac{\gamma_2^{(0)}}{\gamma_2^{(0)} + 2\beta_0} \frac{7}{6} \left(1 - \frac{1}{5}\beta_0 \right) \right], \end{aligned} \quad (2.13)$$

where the anomalous dimension matrix elements are given by $\gamma_1^{(0)} = -\frac{64}{9}$, $\gamma_2^{(0)} = -\frac{100}{9}$ for one-loop order, and $\gamma_1^{(1)} = -\frac{15808}{243}$, $\gamma_2^{(1)} = -\frac{22000}{243}$ for two-loop order. We set $n_f = 5$ for each number.

3 Soft, Collinear and UV divergence

3.1 Soft and collinear divergence cancelation

The soft divergences can occur when the loop momentum l goes to 0. The collinear divergences can arise when l becomes collinear to the momentum of the massless quark q or q' . All these soft and collinear divergences should be canceled out in order to verify that the QCDF framework is valid. In this subsection we explicitly show that the soft and collinear divergences of the order α_s^2 correction for magnetic penguin operator are canceled out in the QCDF framework.

First, we examine the soft divergence cancelation. We set the loop momentum $l \sim \lambda$ where λ is approximately 0 which can be used for investigating the degree of soft divergence. In this way we can easily check the soft divergence by counting the power of λ in the integral. We note that $d^4l \sim \lambda^4$. If the power of λ is smaller than or equal to 0, the integration has soft divergence.

It turns out that the diagrams (1e), (1f), (2) and (5a), (5b), \dots , (7d) have no soft divergences. The soft divergence of the diagram (3) vanishes due to the on-shell condition.

The discussion about the diagram (4) will be done in the later part of this section. We now consider diagrams (1a) and (1b). Except overall factor including color factor (if not mentioned, we imply this suppression below), their integrand is

$$(1a) + (1b) = \frac{1}{l^2((l+p)^2 - m_b^2)} \left(\frac{[\gamma^\nu(\not{l} + u\not{q})\Gamma_{q'}^\mu(\not{l} + \not{p} + m_b)\gamma_\nu][\gamma_\mu]}{q'^2(l+uq)^2} - \frac{[\Gamma_{l+q'}^\mu(\not{l} + \not{p} + m_b)\gamma^\nu][\gamma_\mu(\not{l} + \bar{u}\not{q})\gamma_\nu]}{(l+q')^2(l+\bar{u}q)^2} \right), \quad (3.1)$$

where we suppress the spinor indices. We use square brackets implying separate spinor indices. $\Gamma_{q'}^\mu$ is a Dirac structure coming from Q_{8g} insertion which is defined by

$$\Gamma_{q'}^\mu = \sigma^{\mu\nu} q'_\nu (1 + \gamma_5). \quad (3.2)$$

After l goes to 0 and doing some Dirac algebra, we easily find the terms in the round brackets cancel each other. Similarly, one can find that the soft divergences from diagrams (1c) and (1d) are also canceled each other. Then, we reach that all the soft divergences are safely canceled.

For the collinear divergence, we first consider the case where loop momentum l becomes collinear to the momentum q of upper side quark lines. We typically decompose l as follows,

$$l = \alpha q + \beta \bar{q} + l_\perp^2, \quad (3.3)$$

where $q = (E, 0, 0, E)$, $\bar{q} = (E, 0, 0, -E)$ and $l_\perp = (0, l_1, l_2, 0)$. E is energy of upper side decaying meson which is approximately $E \sim m_b/2$. Because l is collinear to q we set the order of each parameter such that $\alpha \sim 1$, $\beta \sim \lambda^2$ and $l_\perp^2 \sim \lambda^2 m_b^2$, where $\lambda \sim \Lambda_{\text{QCD}}/m_b$. We note that $d^4l = 1/2 dl_q dl_{\bar{q}} dl_\perp^2 \sim \lambda^4 m_b^4$ and $l^2 \sim \lambda^2 m_b^2$. Then we count the power of λ in the integral which implies the degree of collinear divergence. Similar to the soft divergence, if the power of λ is less than or equal to 0, the integral has collinear divergence. One may simply check the collinear divergences from the fact that the gluon, which is connected any one of the external massless quark line, potentially has collinear divergence.

It is simple to find that the diagrams (2), (5a), (5b), \dots , (7c) have no collinear divergence. It is worth showing the integrand of diagram (7d) for studying the collinear divergence:

$$(7d) = \frac{[\tilde{\Gamma}^{\mu\nu}][\gamma_\nu \not{l} \gamma_\mu]}{l^2(l+\bar{u}q)^2(l-p')^2}, \quad (3.4)$$

where $\tilde{\Gamma}^{\mu\nu}$ is the Dirac structure from the qqg vertex of Q_{8g} which is defined by

$$\tilde{\Gamma}^{\mu\nu} = \sigma^{\mu\nu} (1 + \gamma_5). \quad (3.5)$$

After substituting l for αq in the numerator and using some Dirac algebra and on-shell condition, we find that the numerator vanishes. Now we consider again diagram (1a) including color factor:

$$(1a) = \left(-\frac{C_F}{2N_c} \right) \frac{1}{q'^2 l^2 (l+uq)^2} \left([\gamma^\nu(\not{l} + u\not{q})\Gamma_{q'}^\mu \frac{1}{\not{l} + \not{p} - m_b} \gamma_\nu][\gamma_\mu] \right). \quad (3.6)$$

After we substitute l for αq and using $q/(\alpha q + \not{p} - m_b) = 1/\alpha$ from the on-shell condition, we arrive at the collinear divergence term $X_{(1a)}$:

$$X_{(1a)} = -\frac{1}{2N_c} \frac{2}{l^2(l+uq)^2} \left(\frac{\alpha+u}{\alpha} \right) P(u), \quad (3.7)$$

where $P(u)$ is LO contribution of magnetic penguin operator defined by $P(u) = C_F[\Gamma_{q'}^\mu][\gamma_\mu]/(\bar{u}m_b^2)$. Similarly, we can find the collinear divergences of diagrams (1d) and (1e):

$$X_{(1d)} = -\frac{1}{2N_c} \frac{2}{l^2(l+uq)^2} \left(\frac{\alpha+u}{\alpha} \right) (-P(u+\alpha)), \quad (3.8)$$

$$X_{(1e)} = \left(\frac{1}{2N_c} + C_F \right) \frac{2}{l^2(l+uq)^2} \left(\frac{\alpha+u}{\bar{u}} \right) (-P(u+\alpha)). \quad (3.9)$$

From the definition of $P(u)$, one can easily find the relation

$$P(u+\alpha) = \frac{\bar{u}}{(\bar{u}-\alpha)} P(u), \quad (3.10)$$

where we used on-shell condition in order to get $[\Gamma_{q'}^\mu] = [\Gamma_{p'}^\mu]$. Using this equation we can find that the collinear divergences proportional to the color factor $1/(2N_c)$ in $X_{(1a)}$, $X_{(1d)}$ and $X_{(1e)}$ are exactly canceled each other. The remaining collinear divergence term is proportional to C_F , and represented by

$$X_{(1a)+(1d)+(1e)} = C_F \frac{2}{l^2(l+uq)^2} \left(\frac{\alpha+u}{\alpha} \right) (P(u) - P(u+\alpha)). \quad (3.11)$$

We also consider the collinear divergences of diagrams (1b), (1c) and (1f), and the calculation is similar to previous one. The result is

$$X_{(1b)+(1c)+(1f)} = C_F \frac{2}{l^2(l+\bar{u}q)^2} \left(\frac{\alpha+\bar{u}}{\alpha} \right) (P(u) - P(u-\alpha)). \quad (3.12)$$

For the diagram (3), if we consider the projection operator eq. (2.11), we get the following collinear divergence term:

$$X_{(3)} = C_F \frac{2l_\perp^2}{l^2(l+uq)^2(l-\bar{u}q)^2} P(u+\alpha). \quad (3.13)$$

After we change α into $-\alpha$ in eq. (3.12) and take apart the propagators in eq. (3.13), we obtain total collinear divergence term combining eqs. (3.11), (3.12) and (3.13):

$$\begin{aligned} X_{\text{tot}} = C_F & \left(\frac{2(\alpha+u)}{\alpha} \frac{1}{l^2(l+uq)^2} - \frac{2(\bar{u}-\alpha)}{\alpha} \frac{1}{l^2(l-\bar{u}q)^2} \right) (P(u) - P(u+\alpha)) \\ & - C_F \frac{l_\perp^2}{q \cdot l} \left(\frac{1}{l^2(l+uq)^2} - \frac{1}{l^2(l-\bar{u}q)^2} \right) P(u+\alpha). \end{aligned} \quad (3.14)$$

As this equation is same to eq. (193) in ref. [7] except $T(u)$ is changed into $P(u)$, this collinear divergence is to be canceled by one-loop correction of meson distribution amplitude. To be self-contained, here we show again how this cancelation take place. There is

missing collinear divergence that comes from the self energy diagrams of upper side quark fields. We find that this additional collinear divergence is given by

$$X_{\text{add}} = -C_F \left(\frac{(\alpha + u)}{u} \frac{1}{l^2(l + uq)^2} - \frac{(\alpha - \bar{u})}{\bar{u}} \frac{1}{l^2(l - \bar{u}q)^2} \right) P(u). \quad (3.15)$$

We add X_{add} to X_{tot} and integrate them over β and l_{\perp} in order to express them as a convolution in α . Using Cauchy's theorem for integration over β and

$$\int \frac{dl_{\perp}^2}{l_{\perp}^2} = 2 \ln \frac{\mu_{\text{UV}}}{\mu_{\text{IR}}}, \quad (3.16)$$

we can find that $X_{\text{tot}} + X_{\text{add}}$ is expressed by

$$X_{\text{tot}} + X_{\text{add}} = C_F \frac{\alpha_s}{\pi} \ln \frac{\mu_{\text{UV}}}{\mu_{\text{IR}}} \int_0^1 dw P(w) V(w, u). \quad (3.17)$$

$V(w, u)$ is the Efremov-Radyushkin-Brodsky-Lepage (ERBL) kernel [25, 26] defined by

$$V(w, u) = \left[\theta(u - w) \frac{w}{u} \left(1 + \frac{1}{u - w} \right) + \theta(w - u) \frac{\bar{w}}{\bar{u}} \left(1 + \frac{1}{\bar{u} - \bar{w}} \right) \right]_+ \quad (3.18)$$

with the following definition

$$[f(w, u)]_+ \equiv f(w, u) - \delta(w - u) \int_0^1 dv f(v, u). \quad (3.19)$$

We note that the NLO contribution of light meson distribution amplitude is expressed by

$$\Phi_M^{(1)}(w) = C_F \frac{\alpha_s}{\pi} \ln \frac{\mu_{\text{UV}}}{\mu_{\text{IR}}} \int_0^1 du V(w, u) \Phi_M^{(0)}(u). \quad (3.20)$$

Therefore, after the convolution with meson distribution amplitude, the total collinear divergence $X_{\text{tot}} + X_{\text{add}}$ in the matrix element is exactly canceled by NLO correction to the meson distribution amplitude in eq. (2.10).

Finally, we consider the collinear divergence that arises when the loop momentum l is collinear to q' . Diagrams (1c), (1d), (1f), (4) and (7d) have this collinear divergence. Without showing the details, it is found that the collinear divergences of diagrams (1c) and (1d) are canceled each other and so do the diagrams (1f) and (7d). The diagram (4) has both soft and collinear divergences. It is straightforward to show that the soft and collinear divergences of diagram (4) are exactly canceled by second term of eq. (2.10) which is contributed by NLO form-factor correction diagram shown in figure 3. The UV divergence of NLO from-factor correction should be canceled by form-factor renormalization.

3.2 Renormalization - UV divergence cancelation

Now we add gluon self-energy diagrams as well as its counter term as shown in figure 4. The third diagram is the counter term for UV cancelation of diagrams (1c) and (1f). Other diagrams that cause UV divergence are diagrams (1a), (1e), (2), (5a), (5b), (6a-6d) and (7a-7c). These diagrams are same with those for calculating operator renormalization constant Z_{88} except right side quark current. Therefore, all these UV divergences are naturally canceled by operator renormalization equation (2.5).

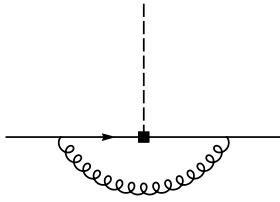


Figure 3. NLO form-factor correction diagram.

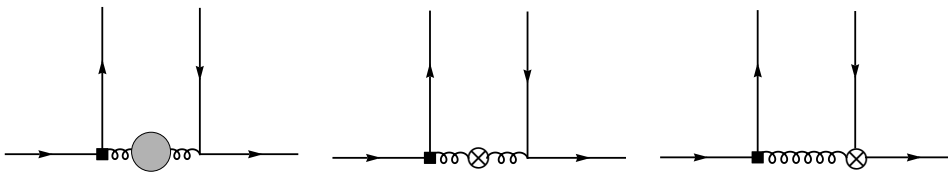


Figure 4. Gluon self-energy diagrams and the counter terms.

4 Result and application

For the calculation, we first reduce the tensor integrals into scalar Feynman integrals. In order to reduce scalar Feynman integrals into the master integrals, we use the Laporta's algorithm [27] with in-house Mathematica code which facilitates several reduction methods such as Passarino-Veltman reduction [28], integration-by-part method [29, 30] and Lorentz-invariance method [31]. We mainly use the Mellin-Barnes representation to compute each master integral. Analytic results of the master integrals are shown in appendix. We explicitly separate the $1/\varepsilon$ and $1/\varepsilon^2$ terms into IR divergence part and UV divergence part by investigating the origin of divergences for each scalar Feynman integral. We confirm that all the IR divergences and UV divergences are canceled separately. Here we show the result of $T_{Q_8}^{(0)}$ and $T_{Q_8}^{(1)}$ (we attach subscript Q_8 in order to denote contribution of magnetic penguin operator) except the color factor C_F/N_c . The LO result $T_{Q_8}^{(0)} = -2/\bar{u}$ is same as in refs. [6, 8].

The NLO result of $T_{Q_8}^{(1)}$ reads as

$$\begin{aligned}
u\bar{u}T_{Q_8}^{(1)} = & \ln\left(\frac{\mu}{m_b}\right) \left(C_F \left(8u \ln(\bar{u}) - \frac{4u}{3} \right) + \frac{8un_f}{3} - \frac{68u}{3N_c} \right) \\
& + i\pi \left(C_F \left(\left(4u - \frac{4\bar{u}}{u^2} \right) \ln(\bar{u}) - \frac{8u}{3} - \frac{4}{u} + 2 \right) \right. \\
& \quad \left. + \frac{1}{N_c} \left(\left(2u - \frac{2}{u^2} \right) \ln(\bar{u}) - \frac{13u}{3} - \frac{2}{u} - 2u \ln(u) - 1 \right) \right) \\
& + C_F \left(\left(\frac{2\bar{u}}{u^2} - 2u \right) \ln^2(\bar{u}) + \left(\frac{8u}{3} + \frac{4}{u} + 2 \right) \ln(\bar{u}) - \frac{88u}{9} + 2 \right) \\
& + \frac{1}{N_c} \left(\left(\frac{2}{u} + 1 - 3u \right) J_1(\bar{u}) - \left(2 + \frac{2}{u} \right) J_2(\bar{u}) - 6u \text{Li}_2(\bar{u}) - 2u \text{Li}_2(u) \right. \\
& \quad \left. + \left(\frac{1}{u^2} + u \right) \ln^2(\bar{u}) - u \ln^2(u) - 4u \ln(\bar{u}) \ln(u) \right. \\
& \quad \left. + \left(\frac{19u}{3} + \frac{2}{u} - 1 \right) \ln(\bar{u}) + 2u \ln(u) + \frac{2\pi^2 u}{3} - \frac{242u}{9} \right) \\
& + (n_f - 2) g_8(0 - i\epsilon, u) + g_8(s_c - i\epsilon, u) + g_8(1, u), \tag{4.1}
\end{aligned}$$

where $s_c = m_c^2/m_b^2$. The definition of $g_8(s, u)$ is

$$g_8(s, u) = \left(\frac{8us}{3\bar{u}} + \frac{4}{3}u \right) J_1\left(\frac{\bar{u}}{s}\right) + \frac{16us}{3\bar{u}} - \frac{4}{3}u \ln(s) + \frac{20u}{9}. \tag{4.2}$$

The function $J_1(\bar{u})$ and $J_2(\bar{u})$ are defined by

$$\begin{aligned}
J_1(\bar{u}) &= \frac{1 + y(\bar{u})}{1 - y(\bar{u})} \ln(y(\bar{u})), \\
J_2(\bar{u}) &= \frac{\text{Li}_2(\bar{u})}{u} - \frac{\pi^2}{6u} - \int_0^1 d\xi \frac{\ln(1 - \bar{u}\xi(1 - \xi))}{(1 - \xi)(1 - \bar{u}\xi)}, \tag{4.3}
\end{aligned}$$

where

$$y(\bar{u}) = \frac{\sqrt{4 - \bar{u}} - \sqrt{-\bar{u}}}{\sqrt{4 - \bar{u}} + \sqrt{-\bar{u}}}. \tag{4.4}$$

In the case $s \rightarrow 0$, we find

$$g_8(0 - i\epsilon, u) = \frac{20u}{9} - \frac{4}{3}u \ln(\bar{u}) + i\pi \frac{4}{3}u. \tag{4.5}$$

Even though $J_2(\bar{u})$ has integral form due to a non-trivial master integral, after convolution with meson distribution amplitude we could obtain complete analytic result of the hard-scattering amplitude. It should be emphasized that $u\bar{u}T_{Q_8}^{(1)}$ has no singularity except log-singularity as $u \rightarrow 0$ nor $u \rightarrow 1$, so that there is no end-point singularity for the convolution with meson distribution amplitude at leading twist.

After convoluting the hard scattering kernels with meson distribution amplitude at leading twist, we are left with following formula:

$$\begin{aligned}
P_{8,M}^{(0)} &\equiv \int_0^1 du T_{Q_8}^{(0)} \Phi_M(u) = -6(1 + \alpha_1^M + \alpha_2^M), \\
P_{8,M}^{(1)} &\equiv \int_0^1 du T_{Q_8}^{(1)} \Phi_M(u) \\
&= 4\pi \text{Cl}_2\left(\frac{2\pi}{3}\right) - 8\text{Cl}_3\left(\frac{2\pi}{3}\right) - \frac{332\zeta(3)}{9} - \frac{10\pi^2}{9} + \frac{11\pi}{\sqrt{3}} - 123 \\
&\quad + \left(16\pi \text{Cl}_2\left(\frac{\pi}{3}\right) - 12\pi \text{Cl}_2\left(\frac{2\pi}{3}\right) - 24\text{Cl}_3\left(\frac{2\pi}{3}\right) + \frac{892\zeta(3)}{3} + \frac{38\pi^2}{3}\right. \\
&\quad \left. - 49\sqrt{3}\pi - \frac{4243}{9}\right) \alpha_1^M + \left(-96\pi \text{Cl}_2\left(\frac{2\pi}{3}\right) + 192\text{Cl}_3\left(\frac{2\pi}{3}\right)\right. \\
&\quad \left. - \frac{3464\zeta(3)}{3} - 60\pi^2 + 257\sqrt{3}\pi + \frac{11011}{18}\right) \alpha_2^M + (n_f - 2)G_8^M(0 - i\epsilon) \\
&\quad + G_8^M(s_c - i\epsilon) + G_8^M(1) + \left(-\frac{236\alpha_1^M}{3} - \frac{308\alpha_2^M}{3} - 36\right) \ln\left(\frac{\mu}{m_b}\right) \\
&\quad + i\pi \left(\left(52\pi^2 - \frac{1747}{3}\right) \alpha_1^{M_2} + \left(\frac{6032}{3} - 212\pi^2\right) \alpha_2^{M_2} - \frac{16\pi^2}{3} + 9\right). \tag{4.7}
\end{aligned}$$

The function $G_8^M(s)$ is defined by

$$\begin{aligned}
G_8^M(s) &= -24s^2 \ln^2(\tilde{y}(s)) + (4 - 40s) \left(\frac{1 + \tilde{y}(s)}{1 - \tilde{y}(s)}\right) \ln(\tilde{y}(s)) - 104s - 4 \ln(s) + \frac{38}{3} \\
&\quad + \alpha_1^M \left(24(8s - 9)s^2 \ln^2(\tilde{y}(s)) - 4(48s^2 + 34s - 1) \left(\frac{1 + \tilde{y}(s)}{1 - \tilde{y}(s)}\right) \ln(\tilde{y}(s))\right. \\
&\quad \left. - 192s^2 - 440s - 4 \ln(s) + 18\right) \\
&\quad + \alpha_2^M \left(-48(45s^2 - 40s + 18) s^2 \ln^2(\tilde{y}(s))\right. \\
&\quad \left. + 4(540s^3 - 390s^2 - 70s + 1) \left(\frac{1 + \tilde{y}(s)}{1 - \tilde{y}(s)}\right) \ln(\tilde{y}(s))\right. \\
&\quad \left. + 2160s^3 - 1740s^2 - 1064s - 4 \ln(s) + 21\right), \tag{4.8}
\end{aligned}$$

where

$$\tilde{y}(s) = \frac{\sqrt{1 - 4s} - 1}{\sqrt{1 - 4s} + 1}. \tag{4.9}$$

In order to obtain the above equation, we use inverse binomial summation formula [32]. The Clausen function $\text{Cl}_n(\theta)$ is defined in terms of poly-logarithm function [33]

$$\text{Cl}_n(x) = \begin{cases} \frac{i}{2} (\text{Li}_n(e^{-i\theta}) - \text{Li}_n(e^{i\theta})) & n \text{ is even} \\ \frac{1}{2} (\text{Li}_n(e^{-i\theta}) + \text{Li}_n(e^{i\theta})) & n \text{ is odd} \end{cases}. \tag{4.10}$$

In eq. (4.7), we explicitly show the imaginary part in the last line. The other sources of imaginary part are $G_8^M(0 - i\epsilon)$ and $G_8^M(s_c - i\epsilon)$. These imaginary parts arise first at NLO

(order α_s^2) for the magnetic penguin operator which causes strong CP phase in non-leptonic B decays.

Now we apply our result to $B \rightarrow K\pi$ decays. They are well studied in ref. [8] within the QCDF framework up to NLO. Here we follow the notation and the formula in ref. [8] for comparing our order α_s^2 result with their NLO one. The $B \rightarrow K\pi$ decay amplitudes $\mathcal{A}(B \rightarrow \pi K)$ without annihilation amplitudes are expressed by

$$\begin{aligned}
\mathcal{A}(B^- \rightarrow \pi^- \bar{K}^0) &= \lambda_p \left[\left(a_4^p - \frac{1}{2} a_{10}^p \right) + r_\chi^K \left(a_6^p - \frac{1}{2} a_8^p \right) \right] A_{\pi K}, \\
-\sqrt{2} \mathcal{A}(B^- \rightarrow \pi^0 K^-) &= [\lambda_u a_1 + \lambda_p (a_4^p + a_{10}^p) + \lambda_p r_\chi^K (a_6^p + a_8^p)] A_{\pi K} \\
&\quad + \left[\lambda_u a_2 + \lambda_p \frac{3}{2} (-a_7 + a_9) \right] A_{K\pi}, \\
-\mathcal{A}(\bar{B}^0 \rightarrow \pi^+ K^-) &= [\lambda_u a_1 + \lambda_p (a_4^p + a_{10}^p) + \lambda_p r_\chi^K (a_6^p + a_8^p)] A_{\pi K}, \\
\sqrt{2} \mathcal{A}(\bar{B}^0 \rightarrow \pi^0 \bar{K}^0) &= \mathcal{A}(B^- \rightarrow \pi^- \bar{K}^0) + \sqrt{2} \mathcal{A}(B^- \rightarrow \pi^0 K^-) \\
&\quad - \mathcal{A}(\bar{B}^0 \rightarrow \pi^+ K^-). \tag{4.11}
\end{aligned}$$

Here, λ_p represents CKM factor defined by $\lambda_p = V_{pb} V_{ps}^*$, and the summation with $p = u, c$ is implicitly considered. It should be emphasized that the terms with λ_u is highly CKM-suppressed as estimated by $|V_{ub} V_{us}^* / V_{cb} V_{cs}^*| \approx 0.02$. $A_{\pi K}$ and $A_{K\pi}$ contain all the hadronic parameters such as form-factor, meson decay constant and mass factor. The dimensionless coefficients a_i represent the hard-scattering contribution of each operator combined with its Wilson coefficient. r_χ^K is chiral-enhancement factor defined by

$$r_\chi^K = \frac{2m_K^2}{\bar{m}_b (\bar{m}_q + \bar{m}_s)}, \tag{4.12}$$

where $q = u$ for charged kaon and $q = d$ for neutral kaon. It is known that a_4^c and $r_\chi^K a_6^c$ make dominant contribution in $B \rightarrow K\pi$ decays among the a_i 's. Both come from the contribution of penguin operators. The magnetic penguin operator contributes to both a_4^c and $r_\chi^K a_6^c$, but with different twist order of light-cone projection operator of pseudoscalar meson: leading twist for a_4^c and twist-3 for $r_\chi^K a_6^c$. Since, up to order α_s , the twist-3 contribution of magnetic penguin operator is quite suppressed than the leading twist contribution, here we only consider NLO contribution of magnetic penguin operator to a_4^c which requires leading twist projection.

Without considering hard spectator scattering term (the term specified $a_{4,\text{II}}^c$), we separate coefficient $a_{4,\text{I}}^c$ (subscript I denotes the hard-scattering form-factor term) into three terms in order to compare the contributions of different sources:

$$a_{4,\text{I}}^c = a_{4,\text{I}}^{c,V} + a_{4,\text{I}}^{c,P} + a_{4,\text{I}}^{c,P_8}, \tag{4.13}$$

where $a_{4,\text{I}}^{c,V}$ denotes vertex correction term, $a_{4,\text{I}}^{c,P}$ represents penguin correction term and $a_{4,\text{I}}^{c,P_8}$ is reserved for magnetic penguin operator contribution. We note that the three quantities are separately gauge-invariant, since they come from different gauge-invariant effective operators. Some care is needed for renormalization scheme dependence in each term. We

Table 1. Input parameters.

Parameters	$\Lambda_{\overline{\text{MS}}}^{(5)}$	$m_b(m_b)$	$m_c(m_b)$	α_1^K (1 GeV)	α_2^K (1 GeV)
Values	225 MeV	4.2 GeV	1.3 ± 0.2 GeV	0.3 ± 0.3	0.1 ± 0.3

see that the vertex correction starts from order unity while the penguin correction as well as the magnetic penguin correction start at α_s , the vertex correction term $a_{4,I}^{c,V}$ makes dominant contribution.

We show again the NLO expressions of each coefficient from ref. [8] including our result of NLO magnetic penguin operator contribution

$$\begin{aligned}
a_{4,I}^{c,V} &= C_4 + \frac{C_3}{N_c} \left(1 + C_F \frac{\alpha_s}{4\pi} \left(12 \ln \frac{m_b}{\mu} - 18 + \int_0^1 du g(u) \Phi_K(u) \right) \right), \\
a_{4,I}^{c,P} &= \frac{C_F \alpha_s}{N_c 4\pi} \left(C_1 \left(\frac{4}{3} \ln \frac{m_b}{\mu} + \frac{2}{3} - G_K(s_c) \right) + C_3 \left(\frac{8}{3} \ln \frac{m_b}{\mu} + \frac{4}{3} - G_K(0) - G_K(1) \right) \right. \\
&\quad \left. + (C_4 + C_6) \left(\frac{4n_f}{3} \ln \frac{m_b}{\mu} - (n_f - 2)G_K(0) - G_K(s_c) - G_K(1) \right) \right), \\
a_{4,I}^{c,P_8} &= C_{8g}^{\text{eff}} \frac{C_F \alpha_s}{N_c 4\pi} \left(P_{8,K}^{(0)} + \left(\frac{\alpha_s}{4\pi} \right) P_{8,K}^{(1)} \right), \tag{4.14}
\end{aligned}$$

where the loop-effect functions $g(u)$, $G_K(s)$ are defined in ref. [8], and the $P_{8,K}^{(0,1)}$ can be read off from eqs. (4.6) and (4.7).

For the numerical analysis, we compare the NLO contribution of magnetic penguin operator with its LO contribution and also with other penguin contribution and vertex contribution up to the NLO. We summarize input parameter values in table 1. We use two-loop running coupling constant and running quark mass with provided parameters. For the Gegenbauer moments, we use the values at the fixed scale with conservatively chosen errors that are consistent with several QCD sum rule results [34, 35]. With this preparation, we compute the values for $a_{4,I}^{c,P_8}$ at the LO and NLO with three different scale values. The result is described in table 2. For comparison, we also show numerical values of the $a_{4,I}^{c,V}$ and $a_{4,I}^{c,P}$ at NLO. The errors propagated from the uncertainties of Gegenbauer moments and charm quark mass are given in the round and square brackets respectively. It should be noted that the contribution of magnetic penguin operator has opposite sign from the vertex and penguin correction, and compensates the other contribution. Specifically, the real value of LO magnetic penguin contribution $a_{4,I}^{c,P_8}$ (order α_s) is comparable to that of NLO penguin contribution $a_{4,I}^{c,P}$ (order α_s) and both cancel each other at $\mu = m_b$. As can be seen, the NLO contribution of magnetic penguin operator is significant and can considerably reduce the absolute value of total coefficient $a_{4,I}^c$. Especially, for the imaginary part, $a_{4,I}^{c,P_8}$ (NLO) contribution is so strong that the contribution significantly reduces the total value. We emphasize that the large NLO contribution is mainly from the order α_s^2 QCD effect of the hard scattering term. We also comment that the contribution from the order α_s^2 hard spectator scattering with QCD penguin contraction is very small, as can be seen in ref. [16].

Table 2. Numerical result of coefficients $a_{4,I}^{c,P_8}$ up to LO and NLO compared with NLO values of $a_{4,I}^{c,V}$ and $a_{4,I}^{c,P}$ at three different scale values. The numbers in round brackets indicate maximal variation due to the uncertainty of Gegenbauer moments while the numbers in square brackets represent the variation from the charm mass uncertainty.

μ	Real part			Imaginary part		
	$m_b/2$	m_b	$2m_b$	$m_b/2$	m_b	$2m_b$
$a_{4,I}^{c,V}$	-0.046(1)	-0.033	-0.024	-0.003(1)	-0.001(1)	-0.001
$a_{4,I}^{c,P}$	-0.003(2)[1]	-0.009(1)[1]	-0.014(1)[1]	-0.001(3)[4]	-0.003(2)[3]	-0.003(2)[3]
$a_{4,I}^{c,P_8}$ (LO)	0.014(2)	0.009(2)	0.007(1)	0	0	0
$a_{4,I}^{c,P_8}$ (NLO)	0.019(4)	0.014(3)	0.010(2)	0.007(2)	0.004(1)	0.002(1)

5 Conclusions

We computed the one-loop (order α_s^2) contribution of magnetic penguin operator for B decays to light meson within the QCDF framework. It is explicitly shown that all the soft and collinear divergences are canceled out. All the results are expressed in complete analytic forms so that they can be easily applied to various non-leptonic B decays. It turns out that the NLO contribution of magnetic penguin operator is quite significant especially for imaginary part in $B \rightarrow K\pi$ decays. Therefore, the missing part of the order α_s^2 correction to the hard-scattering form-factor term for penguin amplitude is strongly required for precise estimates of CP asymmetries. It is interesting that the order α_s^2 contribution of magnetic penguin operator considerably reduces the absolute value of penguin amplitude coefficient a_4^c . Combining future analysis for the order α_s^2 penguin correction together with the current result of order α_s^2 vertex correction and hard-spectator scattering corrections, we could reach at the complete order α_s^2 accuracy for $B \rightarrow K\pi$ decays at the leading power of Λ_{QCD}/m_b .

A Appendix: Analytic formulae of the master integrals

In this section, we summarize the result on the computation of the master integrals. We end up with 8 master integrals which are displayed in figure 5. The calculation is based on $\overline{\text{MS}}$ renormalization scheme. Our convention for the master integral with propagators $\mathcal{P}_1, \mathcal{P}_2, \dots, \mathcal{P}_n$ is

$$(\mu e^{\gamma_E/2})^{4-d} \int \frac{d^d l}{i\pi^{d/2}} \frac{1}{\mathcal{P}_1 \mathcal{P}_2 \cdots \mathcal{P}_n}. \quad (\text{A.1})$$

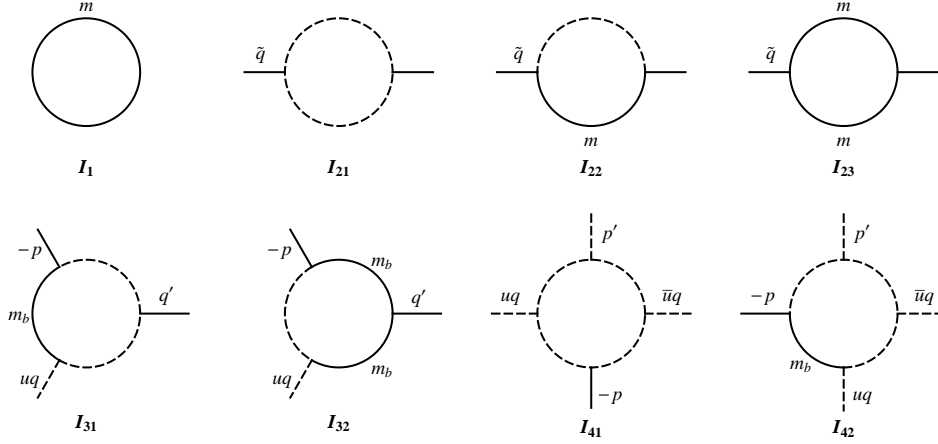


Figure 5. Master Integrals. Solid line represents ‘massive’ for propagator whose mass is explicitly shown in the diagram, and non-zero virtuality for external line. Dashed line implies massless propagator or zero virtuality. All the momenta are understood to be ingoing.

$$I_1 = -m^2 \left(\frac{\mu^2}{m^2} \right)^\varepsilon (e^{\gamma_E \varepsilon}) \Gamma(-1 + \varepsilon). \quad (\text{A.2})$$

$$I_{21} = \left(\frac{\mu^2}{-\tilde{q}^2} + i0 \right)^\varepsilon (e^{\gamma_E \varepsilon}) \frac{\Gamma(1 - \varepsilon)^2 \Gamma(\varepsilon)}{\Gamma(2 - 2\varepsilon)}. \quad (\text{A.3})$$

$$I_{22}(\tilde{q}^2 < m^2) = \left(\frac{\mu^2}{m^2} \right)^\varepsilon \left[2 - \frac{(x+1) \ln(x+1)}{x} + \frac{1}{\varepsilon} + \varepsilon \left(\left(\frac{1}{x} + 1 \right) \text{Li}_2(-x) \right. \right. \\ \left. \left. + \left(\frac{1}{x} + 1 \right) \ln^2(x+1) - \frac{2(x+1) \ln(x+1)}{x} + \frac{\pi^2}{12} + 4 \right) + \mathcal{O}(\varepsilon^2) \right], \\ \text{where } x = -\frac{\tilde{q}^2}{m^2}, \quad (\text{A.4})$$

$$I_{22}(\tilde{q}^2 = 0) = \left(\frac{\mu^2}{m^2} \right)^\varepsilon \left[\frac{1}{\varepsilon} + 1 + \varepsilon \left(1 + \frac{\pi^2}{12} \right) + \mathcal{O}(\varepsilon^2) \right]. \quad (\text{A.5})$$

$$I_{23} = \left(\frac{\mu^2}{m^2} \right)^\varepsilon \left[\frac{1}{\varepsilon} + 2 + \frac{1 + y(-x)}{1 - y(-x)} \ln(y(-x)) + \mathcal{O}(\varepsilon) \right]. \quad (\text{A.6})$$

$$I_{31} = \frac{1}{m_b^2} \left(\frac{\mu^2}{m_b^2} \right)^\varepsilon \left[-\frac{1}{2u} \left((\ln(\bar{u}) - i\pi)^2 + \pi^2 \right) + \mathcal{O}(\varepsilon) \right]. \quad (\text{A.7})$$

$$I_{32} = \frac{1}{m_b^2} \left(\frac{\mu^2}{m_b^2} \right)^\varepsilon \left[\frac{\text{Li}_2(\bar{u})}{u} - \frac{\pi^2}{6u} - \int_0^1 d\xi \frac{\ln(1 - \bar{u}\xi(1 - \xi))}{(1 - \xi)(1 - \bar{u}\xi)} + \mathcal{O}(\varepsilon) \right]. \quad (\text{A.8})$$

$$I_{41} = \frac{1}{m_b^4} \left(-\frac{\mu^2}{m_b^2} + i0 \right)^\varepsilon \frac{1}{u\bar{u}} \left[\frac{2}{\varepsilon^2} - \frac{2 \ln(u\bar{u})}{\varepsilon} \right. \\ \left. - 2\text{Li}_2(u) - 2\text{Li}_2(\bar{u}) + \ln^2\left(\frac{\bar{u}}{u}\right) + \frac{\pi^2}{6} + \mathcal{O}(\varepsilon) \right]. \quad (\text{A.9})$$

$$I_{42} = \frac{1}{m_b^4} \left(\frac{\mu^2}{m_b^2} \right)^\varepsilon \frac{1}{\bar{u}} \left[-\frac{3}{2\varepsilon^2} + \frac{\ln(\bar{u}) - i\pi}{\varepsilon} + \frac{13\pi^2}{24} + \mathcal{O}(\varepsilon) \right]. \quad (\text{A.10})$$

We note that maintaining integral form in I_{32} is convenient for convolution with meson distribution amplitude.

Acknowledgments

Y.W.Y thanks KIAS Center for Advanced Computation for providing computing resources. The work of C.S.K. was supported by the NRF grant funded by the Korea government (MEST) (No. 2011-0027275) and (No. 2011-0017430).

References

- [1] S. W. Lin *et al.* [The Belle Collaboration], *Difference in direct charge-parity violation between charged and neutral B meson decays*, Nature **452**, 332 (2008).
- [2] B. Aubert *et al.* [BABAR Collaboration], *Study of $B^0 \rightarrow \pi^0\pi^0$, $B^\pm \rightarrow \pi^\pm\pi^0$, and $B^\pm \rightarrow K^\pm\pi^0$ decays, and isospin analysis of $B \rightarrow \pi\pi$ decays*, Phys. Rev. D **76**, 091102 (2007) [arXiv:0707.2798].
- [3] B. Aubert *et al.* [BABAR Collaboration], *Observation of CP violation in $B^0 \rightarrow K^+\pi^-$ and $B^0 \rightarrow \pi^+\pi^-$* , Phys. Rev. Lett. **99**, 021603 (2007) [arXiv:hep-ex/0703016].
- [4] T. Aaltonen *et al.* [CDF Collaboration], *Measurements of direct CP violating asymmetries in charmless decays of strange bottom mesons and bottom baryons*, Phys. Rev. Lett. **106**, 181802 (2011) [arXiv:1103.5762].
- [5] S. Perazzini [LHCb Collaboration], *Measurements of $A_{CP}(B^0 \rightarrow K^+\pi^-)$ and $A_{CP}(B_s \rightarrow \pi^+K^-)$ at LHCb*, [arXiv:1106.1197].
- [6] M. Beneke, G. Buchalla, M. Neubert and C. T. Sachrajda, *QCD factorization for $B \rightarrow \pi\pi$ decays: Strong phases and CP violation in the heavy quark limit*, Phys. Rev. Lett. **83**, 1914 (1999) [arXiv:hep-ph/9905312].
- [7] M. Beneke, G. Buchalla, M. Neubert and C. T. Sachrajda, *QCD factorization for exclusive, nonleptonic B meson decays: General arguments and the case of heavy light final states*, Nucl. Phys. B **591**, 313 (2000) [arXiv:hep-ph/0006124].
- [8] M. Beneke, G. Buchalla, M. Neubert and C. T. Sachrajda, *QCD factorization in $B \rightarrow \pi K, \pi\pi$ decays and extraction of Wolfenstein parameters*, Nucl. Phys. B **606**, 245 (2001) [arXiv:hep-ph/0104110].
- [9] M. Beneke and M. Neubert, *QCD factorization for $B \rightarrow PP$ and $B \rightarrow PV$ decays*, Nucl. Phys. B **675**, 333 (2003) [arXiv:hep-ph/0308039].
- [10] G. Bell, *NNLO vertex corrections in charmless hadronic B decays: Imaginary part*, Nucl. Phys. B **795**, 1 (2008) [arXiv:0705.3127].
- [11] G. Bell, *NNLO vertex corrections in charmless hadronic B decays: Real part*, Nucl. Phys. B **822**, 172 (2009) [arXiv:0902.1915].
- [12] M. Beneke, T. Huber and X. Q. Li, *NNLO vertex corrections to non-leptonic B decays: Tree amplitudes*, Nucl. Phys. B **832**, 109 (2010) [arXiv:0911.3655].
- [13] M. Beneke and S. Jager, *Spectator scattering at NLO in non-leptonic b decays: Tree amplitudes*, Nucl. Phys. B **751**, 160 (2006) [arXiv:hep-ph/0512351].

- [14] V. Pilipp, *Hard spectator interactions in $B \rightarrow \pi\pi$ at order α_s^2* , Nucl. Phys. B **794**, 154 (2008) [arXiv:0709.3214].
- [15] N. Kivel, *Radiative corrections to hard spectator scattering in $B \rightarrow \pi\pi$ decays*, JHEP **0705**, 019 (2007) [arXiv:hep-ph/0608291].
- [16] M. Beneke and S. Jager, *Spectator scattering at NLO in non-leptonic B decays: Leading penguin amplitudes*, Nucl. Phys. B **768**, 51 (2007) [arXiv:hep-ph/0610322].
- [17] A. Jain, I. Z. Rothstein and I. W. Stewart, *Penguin loops for nonleptonic B -decays in the standard model: Is there a penguin puzzle?*, [arXiv:0706.3399].
- [18] G. Buchalla, A. J. Buras and M. E. Lautenbacher, *Weak decays beyond leading logarithms*, Rev. Mod. Phys. **68**, 1125 (1996) [arXiv:hep-ph/9512380].
- [19] B. Grinstein, R. P. Springer and M. B. Wise, *Strong interaction effects in weak radiative anti- B meson decay*, Nucl. Phys. B **339**, 269 (1990).
- [20] K. G. Chetyrkin, M. Misiak and M. Munz, *Weak radiative B meson decay beyond leading logarithms*, Phys. Lett. B **400**, 206 (1997) [Erratum-ibid. B **425**, 414 (1998)] [arXiv:hep-ph/9612313].
- [21] C. Greub and P. Liniger, *Calculation of next-to-leading QCD corrections to $b \rightarrow sg$* , Phys. Rev. D **63**, 054025 (2001) [arXiv:hep-ph/0009144].
- [22] E. G. Floratos, D. A. Ross and C. T. Sachrajda, *Higher order effects in asymptotically free gauge theories: The anomalous dimensions of wilson operators*, Nucl. Phys. B **129**, 66 (1977) [Erratum-ibid. B **139**, 545 (1978)].
- [23] A. Gonzalez-Arroyo, C. Lopez and F. J. Yndurain, *Second order contributions to the structure functions in deep inelastic scattering. 1. Theoretical calculations*, Nucl. Phys. B **153**, 161 (1979).
- [24] D. Mueller, *Conformal constraints and the evolution of the nonsinglet meson distribution amplitude*, Phys. Rev. D **49**, 2525 (1994).
- [25] A. V. Efremov and A. V. Radyushkin, *Factorization and asymptotical behavior of pion form-factor in QCD*, Phys. Lett. B **94**, 245 (1980).
- [26] G. P. Lepage and S. J. Brodsky, *Exclusive processes in perturbative quantum chromodynamics*, Phys. Rev. D **22**, 2157 (1980).
- [27] S. Laporta, *High precision calculation of multiloop Feynman integrals by difference equations*, Int. J. Mod. Phys. A **15**, 5087 (2000) [arXiv:hep-ph/0102033].
- [28] G. Passarino and M. J. G. Veltman, *One loop corrections for e^+e^- annihilation into $\mu^+\mu^-$ in the Weinberg model*, Nucl. Phys. B **160**, 151 (1979).
- [29] F. V. Tkachov, *A theorem on analytical calculability of four loop renormalization group functions*, Phys. Lett. B **100** (1981) 65.
- [30] K. G. Chetyrkin and F. V. Tkachov, *Integration by parts: The algorithm to calculate beta functions in 4 loops*, Nucl. Phys. B **192** (1981) 159.
- [31] T. Gehrmann and E. Remiddi, *Differential equations for two loop four point functions*, Nucl. Phys. B **580**, 485 (2000) [arXiv:hep-ph/9912329].
- [32] A. I. Davydychev and M. Y. Kalmykov, *Massive Feynman diagrams and inverse binomial sums*, Nucl. Phys. B **699**, 3 (2004) [arXiv:hep-th/0303162].

- [33] L. Lewin, *Polylogarithms and associated functions*, North-Holland, Amsterdam, (1981).
- [34] A. Khodjamirian, T. Mannel and M. Melcher, *Kaon distribution amplitude from QCD sum rules*, Phys. Rev. D **70**, 094002 (2004) [arXiv:hep-ph/0407226].
- [35] P. Ball and M. Boglione, *SU(3) breaking in K and K* distribution amplitudes*, Phys. Rev. D **68**, 094006 (2003) [arXiv:hep-ph/0307337].